CHARATERISATION AND MODELLING OF THE HIGHLY DYNAMIC DEFORMATION AND FAILURE BEHAVIOR OF PREVIOUSLY FATIGUED 3D TEXTILE COMPOSITES

W. Hufenbach, M. Gude, R. Protz*
TU Dresden, Institute of Lightweight Engineering and Polymer Technology (ILK),
Holbeinstr. 3, 01307 Dresden, Germany
*Corresponding author (r.protz@ilk.mw.tu-dresden.de)

Keywords: *non-crimp textile composites, glass fiber, fatigue damage behavior, strain rate, damage modelling*

1 Introduction

Non-crimp fabric composites (NCF-composites) offer high specific stiffness and strength as well as an adjustable energy absorption capacity. Thus, they are ideally suited for applications in machine building, vehicle constructions, wind power technology and aviation. For the development of efficient lightweight structures realistic models for anisotropic materials are necessary. For quasi-statically loaded anisotropic materials failure models e. g. by PUCK and CUNTZE are available [1, 2]. The strain rate dependent failure and degradation behavior, in particular of textile-reinforced composites, under highly dynamic loading has been investigated rudimentarily only [3, 4]. Corresponding models for the fatigue prediction of lightweight structures are the focus of numerous research activities (see e.g. [5-7]).

In material modelling usually a defect free material is assumed. In practice, often occurring production and operational related defects (e.g. pores, fatigue or impact damage) are mostly considered globally using safety factors which often lead to oversizing [8]. Several non-destructive techniques are potentially able of detecting defects, but just the exact knowledge of the effects of defects allows the definition of thresholds for product quality. Here, extensive experimental and theoretical studies on glass fibre NCF reinforced epoxy composites (GF-NCF/EP) are performed. The focus is put on the influence of fatigue related predamage under subsequent highly-dynamic tensile loading.

2 Experimental procedures

2.1 Specimen preparation and fatigue predamage

For the experimental and theoretical studies, composites with GF-NCF reinforcement of eight layers [0/45/90/-45/45/90/-45/0] are considered. The plies contain different amount of fibers (49 % in 0°, 23 % in 45°, 23 % in -45 and 5 % in 90°). Using the vacuum assisted resin transfer moulding (VARTM) method, test plates were infiltrated in a flat steel mould with injection resin RIMR 135 with hardener RIMH 134 and RIMH 137 in a ratio of 100:21:9. The mould was evacuated before and during infiltration process in order to avoid pores and to guarantee high quality specimens. After infiltration and hardening test specimens with dimensions of 250 *mm* in length, 25 *mm* in width and 2 *mm* in thickness were cut from the test plate in angles of 0°, 45° and 90° by water jet cutting. For the assessment of the fatigue related predamage on the material behaviour specimens have been fatigued with a uniaxial cyclic testing machine INSTRON model PSB 100. Constant amplitude under pulsating tensile loading (sine wave load cycles) with a load ratio R = 0.1 and a maximum stress of 78.5 *MPa* at a frequency of 6 *Hz* under room temperature was employed. The tests are stopped for a part of specimen at 50.000 cycles and a further part at 75.000 cycles whereat 100.000 cycles is the life time at this maximum stress. The extent of damage before the subsequent highly dynamic test is characterized by non-destructive testing.

2.2 Test and measuring equipment for highly dynamic tensile tests

For the characterization of materials at high loading speeds a servohydraulic high velocity test system (SHP) INSTRON VHS 160/20 is used. The SHP enables tests of materials and components at high deformation speeds of up to 20 *m/s* and a maximum force of 160 *kN*. An upper clamping device "quick grabber", specially adapted to highly dynamic tests, guarantees an impulse-like and rebound-free introduction of forces in tensile tests, as well as constant strain rates during the loading period. The influence of the strain rate on the deformation and failure behavior was studied in the highly dynamic tests for strain rates in the range between 0.0004 s^{-1} and 4 s^{-1}. Aside from machine-integrated measuring equipment for recording the machine path, the force and effective acceleration, an optical measurement device is used for the analysis of the deformation and failure behavior. Therefore the specimens are marked with a dot pattern, whose displacement is recorded with a high speed camera with maximum frame of up to 200.000 images per second. Subsequently the deformation will be analyzed using the ARAMIS software. Additional for the failure analysis of defect containing textile composites, the temperature change in the specimen while being loaded can be recorded using an in-situ high-speed thermograph device.

3 Experimental results

Typical polar diagrams of the Young's modulus dependent on the strain rate for defect-free specimen, which are used as references in the future are shown in Fig. 1. An increase in the Young's modulus with rising load speed can be recognized.

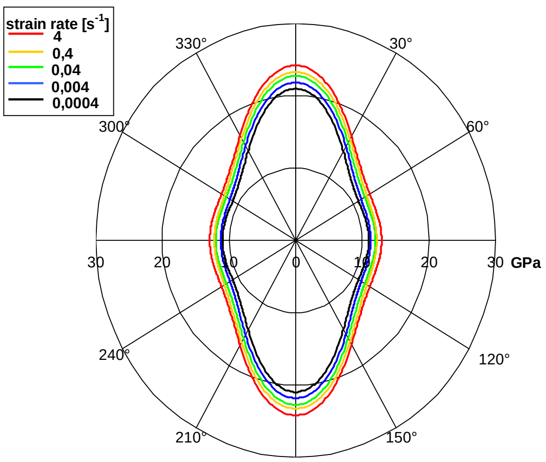

Fig. 1. Strain rate dependent Young`s modulus of GF-NCF/EP

Based on the material behavior under quasistatic loading conditions, to highly dynamic loads, strongly strain rate dependent tensile strengths were determined (Fig. 2). The increase of strength can be quantified with up to 65 % in the considered strain range. The strength increase rate for the 90°-specimens is the lowest with 25 %, which is reasoned in the lower fiber volume fraction in 90° direction.

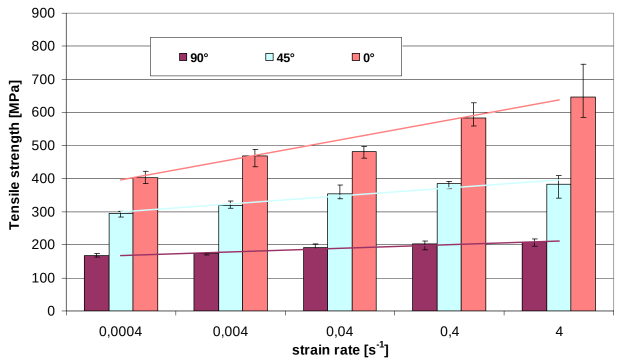

Fig. 2. Average strain rate dependent tensile strength of GF-NCF/EP

Further studies on 90°-specimens show the influence of fatigue predamages on the material behavior of under subsequent high dynamic tensile loading. In particular, a drop of strength but an increase with progressive strain rate can be observed (Fig. 3).

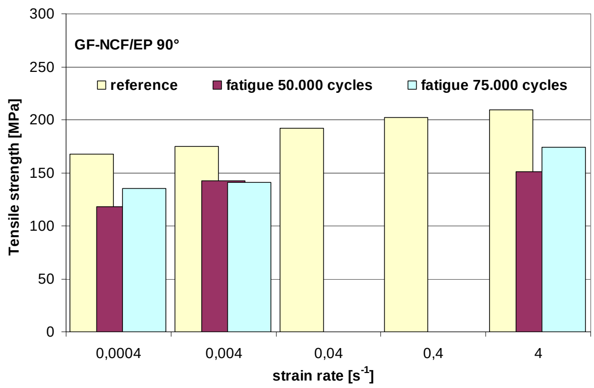

Fig. 3. Average strain rate dependent tensile strength of GF-NCF/EP with and without fatigue predamage in 90° loading direction

For the detailed analysis of the failure behavior and to localize the beginning of failure an in situ high-speed thermography device is used. Due to the high speed rates the arising thermal energy cannot be fully transferred to the environment and a change-over from an isothermal to an adiabatic deformation process takes place. A temperature rise in the composite specimen has been qualitatively monitored and a clear local increase of the temperature especially in the area of the first failure has been observed. As an example a thermo-picture result of highly dynamic process induced failures in the high speed tensile test is shown in Fig. 4 for GF-NCF/EP without and with fatigue predamage at the same strain rate. Composite samples without and with fatigue predamage have a comparable temperature distribution and a uniformly distributed energy dissipation under loading conditions. The fatigue predamaged specimens tend to have lower local sample temperature in comparison to defect free samples loaded under same conditions (Fig. 5).

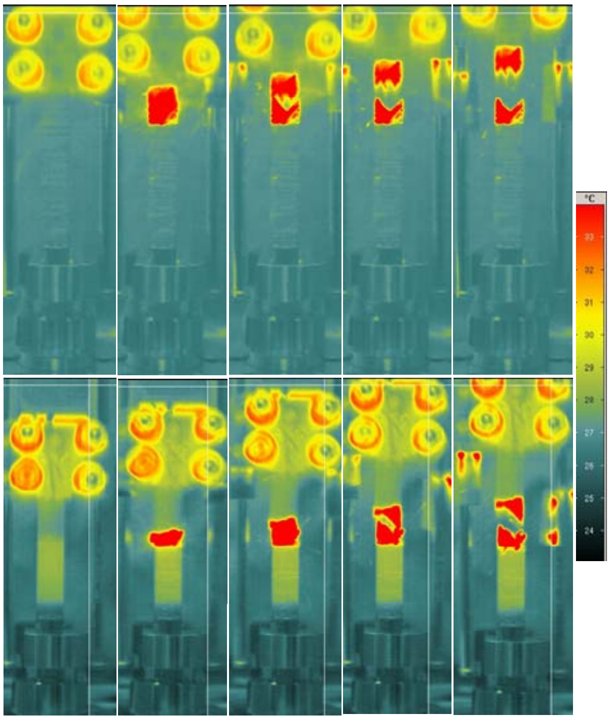

Fig. 4. Images of in-situ high-speed thermograph for analyzing the damage behavior of GF-NCF/EP specimens during highly dynamic loading at constant strain rate of 4 s^{-1} without (top) and with fatigue predamage (bottom)

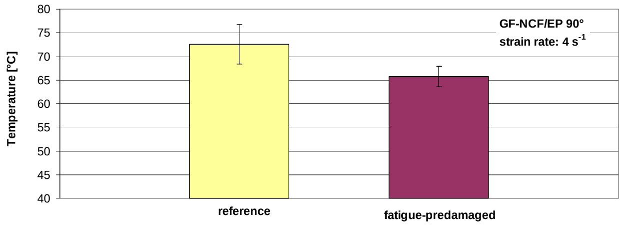

Fig. 5. Maximal temperature of GF-NCF/EP specimen during high-dynamic loading at a constant strain rate of 4 s^{-1} with and without fatigue related predamage

4 Additive damage model

For the mathematical description of the strain rate dependent material behavior of textile reinforced composites with defects resulting from previously fatigue a model is developed, in which the stiffnesses and compliances respectively are described dependent on the strain rate and the extent of material damage by means of a strain rate dependent damage tensor M in the sense of continuum damage mechanics. From a macroscopic point of view, the relation between the nominal stress σ and the effective stress $\tilde{\sigma}$ can be stated as

$$\tilde{\sigma} = M\sigma \qquad (1)$$

with

$$\mathbf{M} = \begin{pmatrix} \frac{1}{1-d_{11}} & 0 & 0 \\ 0 & \frac{1}{1-d_{22}} & 0 \\ 0 & 0 & \frac{1}{1-d_{12}} \end{pmatrix} \qquad (2)$$

Here, the damage parameters

$$\mathbf{D} = \begin{pmatrix} d_{11} \\ d_{22} \\ d_{12} \end{pmatrix} \qquad (3)$$

describe the degree of damage, which depend on the current state of stress, the stress history as well as primarily induced defects.

The damage is described by adapted evolution equations according to

$$\dot{D}_i = D_i^{hd(1)} \cdot \dot{\varepsilon}_i + D_i^{hd(0)} \cdot \dot{\varepsilon}_i^{\lambda_i} \qquad (4)$$

with the strain rates $\dot{\varepsilon}_i = \left[\dot{\varepsilon}_{11}\ \dot{\varepsilon}_{22}\ \dot{\varepsilon}_{12}\right]^{\mathrm{T}}$ and the model parameters $D^{hd(0)}$, $D^{hd(1)}$ for highly dynamic damage and λ_i ($i = 1,2,3$). The damage parameters can be determined, assuming a constant strain rate, by integration over time according to

$$D_i = \left(D_i^{hd(1)} + D_i^{hd(0)} \dot{\varepsilon}^{\lambda_i - 1}\right) \varepsilon_i + D_i^{(2)} \qquad (5)$$

with integration constants $D_i^{(2)}$. From the initial conditions

$$D_i \mid_{\varepsilon=0} = 0 \qquad (6)$$

in the case of a defect free reference state $D_i^{(2)} = 0$ can be obtained. For previously fatigued composites with defined predamage expressed in a additive term $D_i^{(2)} = D_i^{cy} \neq 0$ must be valid.

As evident from the experimental material-mechanical characterizations, the direction related initial modulus of elasticity and thus the compliances are dependent on the strain rate.

With the aid of the non-linear relation

$$\mathrm{E}_{\mathrm{i}}^{(0)}\left(\dot{\varepsilon}_{\mathrm{i}}\right) = \mathrm{E}_{\mathrm{i}}^{(0,\mathrm{ref})}\left[1 + \mathrm{A}_{\mathrm{i}}^{\mathrm{E}} \ln\left(\frac{\dot{\varepsilon}_{\mathrm{i}}}{\dot{\varepsilon}_{\mathrm{i}}^{(\mathrm{ref})}}\right)\right] \qquad (7)$$

and $\mathrm{E}_{\mathrm{i}}^{(0,\mathrm{ref})} = \left[\mathrm{E}_1^{(0,\mathrm{ref})}\ \mathrm{E}_2^{(0,\mathrm{ref})}\ \mathrm{G}_{12}^{(0,\mathrm{ref})}\right]^{\mathrm{T}}$ as – at the respective reference strain rate $\dot{\varepsilon}_{\mathrm{i}}^{(\mathrm{ref})}$ – determined Young's moduli and shear modulus in undamaged state and $\mathrm{A}_{\mathrm{i}}^{\mathrm{E}}$ as material constant, the strain rate dependence of the engineering constant can be described in general.

Together with (5), this results, in the elementary case of a highly dynamic single-axis load under disregard of the influence of the transversal contraction, in the relation

$$\sigma_i = \left[1 - \left(D_i^{(1)} + D_i^{(0)} \dot{\varepsilon}_i^{\lambda_i - 1}\right) \varepsilon_i + D_i^{(ref)}\right] \cdot E_i^{(0,\mathrm{ref})}\left[1 + A_i^E \ln\left(\frac{\dot{\varepsilon}_i}{\dot{\varepsilon}_i^{\mathrm{ref}}}\right)\right] \varepsilon_i \qquad (8)$$

for the calculation of strain rate and damage dependent stress-strain behavior of textile reinforced composites.

The associated direction related material properties and model parameters are determined suitably from highly dynamic experimental investigations for different strain rates by means of inverse parameter identification (table 1).

Here, the model parameters were determined in high speed tensile tests of GF/NCF-EP composites in 0°, 45° and 90° direction without and with fatigue predamage for strain rates in the range between 0.0004 s^{-1} and 0.004 s^{-1}. The model validation was done by experiments with strain rates between 0.04 s^{-1} and 4 s^{-1}.

	Parameter	90°	45°	0°
	$E_i^{(0,\mathrm{ref})}$ $[GPa]$	10,26	14,9	21,15
	$\dot{\varepsilon}_i^{(ref)}$ $[s^{-1}]$	0,0004	0,0004	0,0004
	A_i^{E}	0,02	0,02	0,004
	$D_i^{hd(0)}$	1	0,0001	0,001
	$D_i^{hd(1)}$	14	10	1
	λ_i	0,9	2	0,3
$D_i^{(2)}$	D_i^{cy} 50.000 cycles	0,05	n.d	n.d
	D_i^{cy} 75.000 cycles	0,11	n.d	n.d

Table.1. Model parameters for strain rate dependent in-plane tensile strengths (n.d.: not defined)

Fig. 6 shows the defect free composite specific comparison of experimentally and mathematically determined stress-strain curves dependent on the strain rate for load directions 0°, 45° and 90°. For loading in 0° direction a nearly linear course can be observed, whereas a strong nonlinear stress-strain behavior can identified for loading in 45° and 90° direction. The mathematically determined curves proved to be in close agreement with the experimentally determined stress-strain curves.

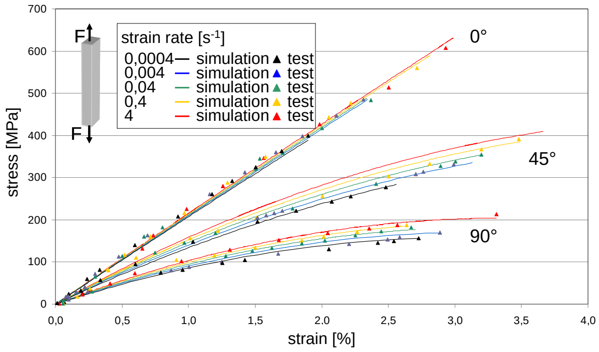

Fig.6. Comparison of experimentally and mathematically determined strain rate dependent stress-strain curves of GF-NCF/EP composites

Fig. 7 shows first results for the influence of fatigue related predamage under subsequent highly dynamic tensile loading for composites in 90° loading direction. The mathematically determined curves also proved a good agreement with the experimentally determined stress-strain curves.

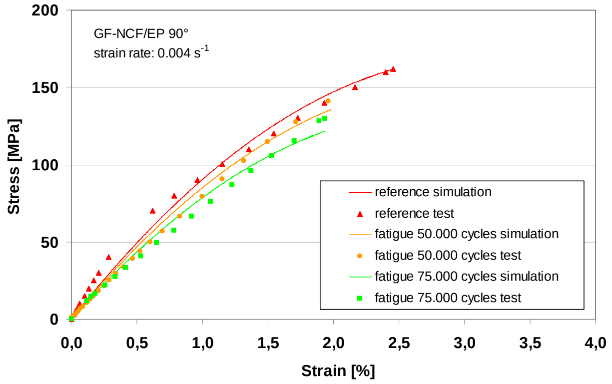

Fig.7. Comparison of experimentally and mathematically determined stress-strain curves of GF-NCF/EP composites at the same strain rate

5 Summary

The design of highly dynamically loaded lightweight components with new types of textile reinforcement requires reliable knowledge of the deformation and failure behavior depending on the loading speed and the fatigue loading history. A servohydraulic high speed test unit in combination with a high-speed camera was used to determine the strain rate dependent material properties of non-crimp glass fiber reinforced composites with fatigue related damage under tensile loading. The deformation and failure behavior of these composites was examined in extensive highly dynamic tensile loading tests. The increase of direction related stiffnesses and strengths at increasing strain rates was successfully quantified on the one hand and the influence of fatigue related damage to subsequent highly dynamic tensile loading was basically characterized. For the mathematical description of the strain rate dependent material behavior of textile reinforced composites with defects resulting from previously fatigue an additive model in the sense of continuum damage mechanics was introduced and validated.

Acknowledgement

The authors gratefully acknowledge the financial support within the scope of research project PAK 267 “Effects of Defects” by the Deutsche Forschungsgemeinschaft (DFG).

References

[1] A. Puck „*Festigkeitsanalyse von Faser-Matrix-Laminaten, Modelle für die Praxis*“ Carl Hanser-Verlag, München 1996.

[2] R. Cuntze, et al. “Neue Bruchkriterien und Festigkeitsnachweise für unidirektionalen Faserkunststoffverbund unter mehrachsiger Beanspruchung-Modellbildung und Experimente-“, *Fortschritt-Berichte*, Reihe 5, Nr. 506, VDI-Verlag, Düsseldorf 1997.

[3] B. Song, W. Chen, T. Weerasooriya “Quasi-Static and Dynamic Compressive Behaviors of a S-2 Glass/SC15 Composite”. *Journal of Composite Materials* 37 (2003) 1723-1743.

[4] Ch. Ebert, W. Hufenbach, A. Langkamp, M. Gude “Modelling of strain rate dependent deformation behaviour of polypropylene”. *Polymer Testing*, 30 (2010) 183-187.

[5] R.P.L. Nijssen “Fatigue Life Prediction and Strength Degradation of Wind Turbine Rotor Blade Composites”. *Dissertation*, Faculty of Aerospace Engineering, Delft University, 2007.

[6] M. Gude, W. Hufenbach, I. Koch “Damage evolution of novel 3D textile reinforced composites under fatigue loading conditions”. *Composites Science and Technology*, 70 (2010) 186-192.

[7] W. Van Paegegem, J. Degrieck, “Modelling damage and permanent strain in fibre-reinforced composites under in-plane fatigue loading”. *Composites Science and Technology*, 63 (2003) 5, 677-694.

[8] R. Protz, W. Hufenbach M. Gude, “Versagens- und Degradationsverhalten von defektbehafteten Textilverbundwerkstoffen unter hochdynamischer Belastung”. *TECHNOMER 2009*, Chemnitz, 2009 (CD-ROM).